Supporting Information

Toro *et al.* 10.1073/pnas.0807448105

SI Text

Microscopy. We performed all microscopy on a DM6000B upright microscope (Leica) fitted with a 100 × 1.46 NA HCX Plan APO oil immersion objective (Leica) and a Hamamatsu C9100 EM CCD camera. Images were acquired using custom software written in Matlab (Mathworks) (M. Fero, R. Gomez-Sjoberg, H.H. McAdams, personal communication).

Synchronization. We grew 30-ml cultures in M2G minimal media to a final optical density below 0.4. We found that for consistent results, especially those presented in Fig. 2*E*, it was crucial for the culture to have been growing exponentially for at least 18 h. We centrifuged the culture (8,000 × *g* for 5 min) and washed the pellet with 2 ml of ice-cold M2 (M2G without glucose but including magnesium sulfate, iron sulfate, and calcium chloride). We performed all subsequent steps on ice or in a cold room at 4°Celsius. We centrifuged (16,000 × *g* for 3 min) and resuspended the pellet in 900 μl of ice-cold M2 plus 900 μl of Percoll (Sigma). Next, we centrifuged at 11,000 × *g* for 20 min and collected the lower band composed of swarmer cells. We then washed out the ludox in two rounds of washing with M2 and centrifugation (8,000 × *g* for 3 min). Finally, we resuspended the pellet in room temperature M2G (0.1–1.0 ml depending on the yield of the synchrony) and spotted a 0.5-μl drop onto a microscopy pad made using a silicone isolator (Sigma). The pad was composed of a 1% agarose solution in M2G. We found that it is important to avoid boiling the agarose solution for too long, presumably because it depletes the dissolved oxygen. We allowed the spotted drop to dry on the pad, covered it with a coverslip and sealed it with a 1:1:1 mixture of paraffin, lanolin, and Vaseline.

Time-Lapse Analysis. Unless stated otherwise in the text, we induced expression of fluorescent proteins driven by the xylose promoter by adding 0.03% xylose (wt/wt) for 75 min before the start of synchrony. In the case of *lacI-CFP* fusions, we also added a final concentration of 50 micromolar Isopropyl β-D-1-thiogalactopyranoside (IPTG) to the liquid culture as well as to all solutions used during the synchrony and to the agarose pad. To avoid phototoxicity effects, we kept the light exposure as low as possible while retaining a good signal-to-noise ratio, and we adjusted the timing of our image acquisition to the onset of segregation in each particular strain to avoid over-sampling. Images were acquired every 5 min.

Image Analysis and Manipulations. We used Photoshop and Image Ready CS2 (Adobe) to make false color merges of captured images, and then used the autolevels and despeckle functions to reduce noise and enhance visibility of foci. The data presented in Figs. 2*E* and 3*B* were counted by hand.

Automated Measurements of Distance-from-the-Pole. The images used for automatic measurements did not undergo the manipulations described above. Instead, we used Matlab version 7.5.0 with the Image Processing, Optimization, and Spline Toolbox for this analysis. We aligned the images from different channels at the pixel level by maximizing the product of the channels. We then located the cells using calibrated thresholding of phase contrast images and determined the subpixel-resolution cell boundaries by interpolation. We defined the poles as the points on the cell boundaries with largest curvature. Next, we drew centerlines that connected the two poles and were equally distant from both cell boundaries. We determined the center of fluorescence peak by fitting a 2D Gaussian to the photon counts in the cell. The distance between the pole and the peak is defined as the length of the centerline between the pole and the projection of the peak center. This code is available upon request.

Recombination. We found that leaky expression from the Pvan promoter was sufficient to induce recombination immediately after transformation of plasmid pTORO78 into cells carrying attP and attB sites. We therefore induced recombination by transforming in the plasmid without adding vanillate. Once a strain had been confirmed as inverted, we stopped selecting for resistance to chloramphenicol to allow for the loss of pTORO78 from the strain.

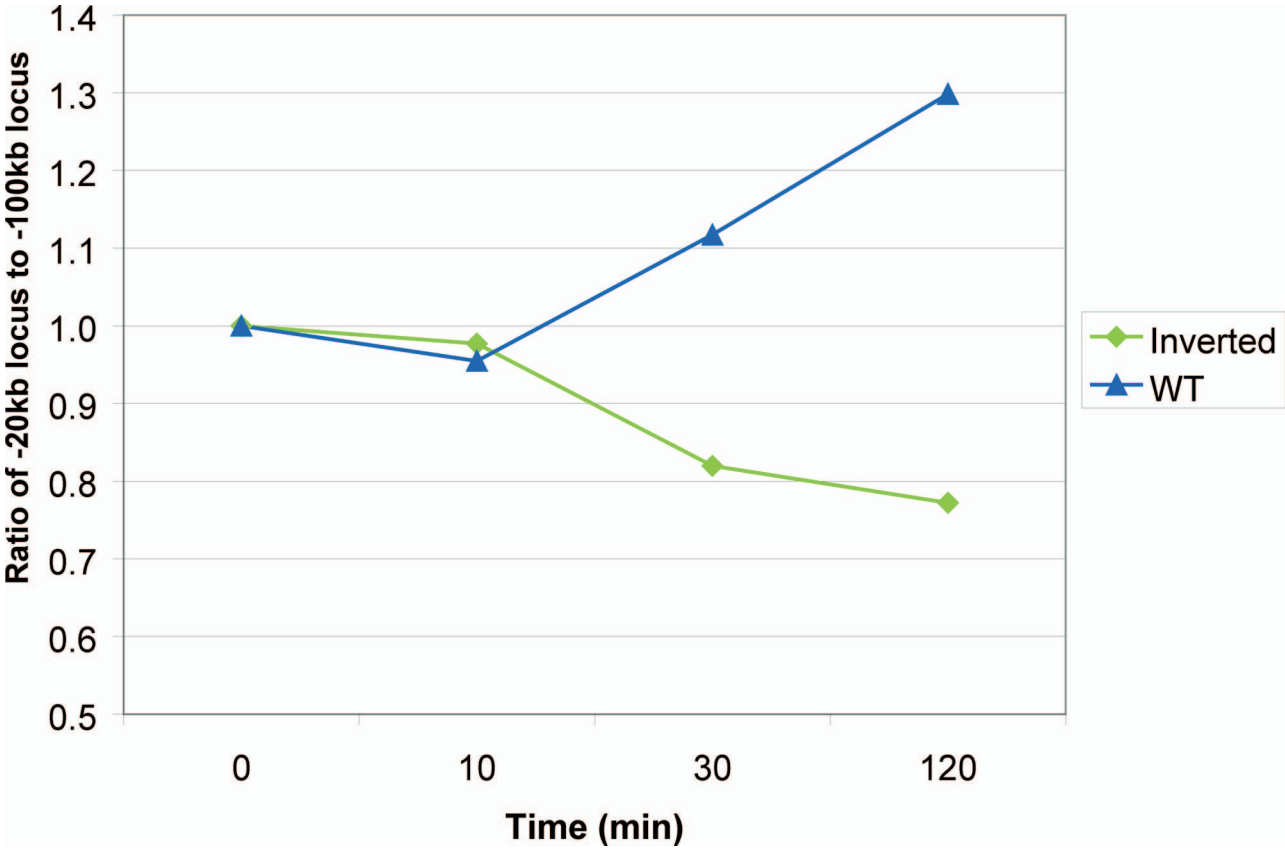

Fig. S1. qPCR of synchronized cells. We designed qPCR Taqman probes (Applied Biosystems) to measure the copy number of DNA located at −20 and −100 kb, inside the borders of the inversion. We then synchronized both WT and inverted strains and took samples at the indicated times. We isolated genomic DNA from each sample and performed qPCR in triplicate according to the manufacturer's instructions. The plot shows the ratio of −20 to −100 kb of DNA as a function of time since synchrony. The ratio between the two loci was normalized to 1 at $t = 0$. It can be seen that in the wild-type strain, as the cell cycle progresses, there is faster accumulation of −20 kb DNA, consistent with this locus being replicated first. In the inverted strain, however, there is faster accumulation of −100 kb DNA and the ratio between −20- and −100-kb drops. This demonstrates that the inverted strain replicates the −100-kb locus before the −20-kb locus and thus confirms the predicted configuration of the inverted chromosome depicted in Fig. 2*D*.

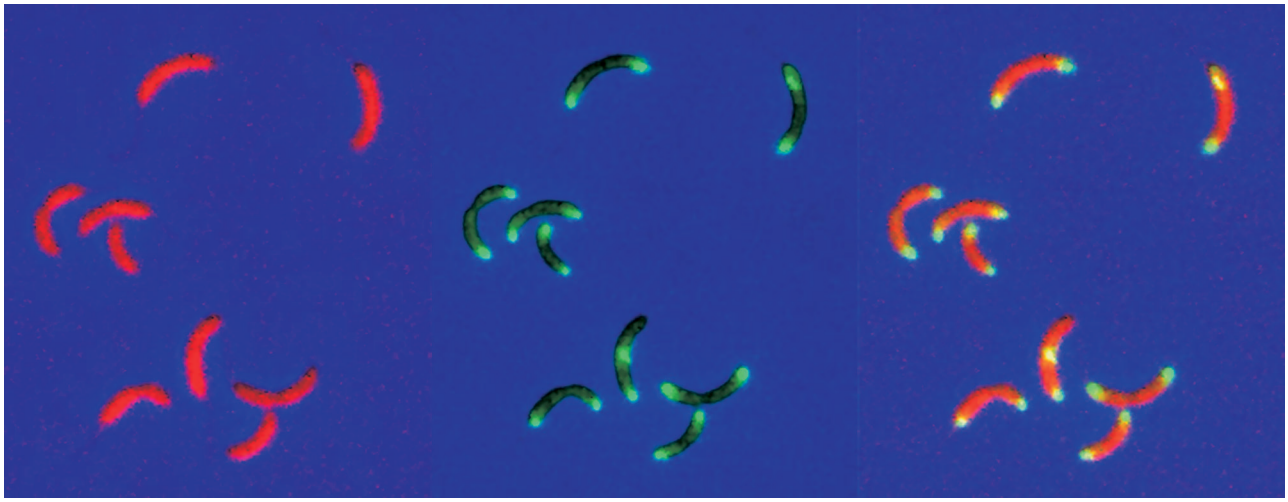

Fig. S2. - Absence of cross-talk between the Caulobacter and pMT1 parS/Micrograph showing the localization of MipZ-YFP and CFP-pMT1Δ,,23ParB in a mixed culture of strain ET150 after 75 min of induction with 0.03% xylose. This strain does not carry a copy of parS(pMT1) in its chromosome. CFP-pMT1Δ23ParB fluorescence (*Left*) pseudocolored red, MipZ-YFP fluorescence (middle) pseudocolored green, and merge (*Right*). All images are overlaid on a blue pseudocolored phase micrograph to show the cell bodies.

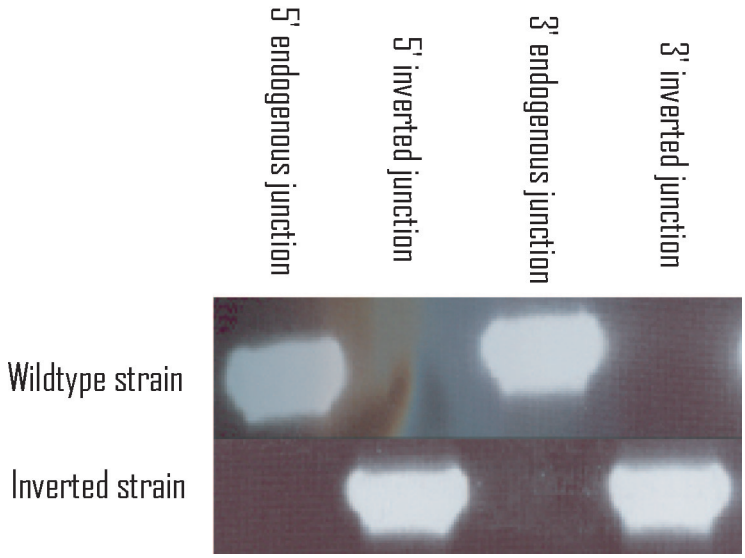

Fig. S3. PCR checks of inverted strains. We designed PCR primers on either side of the PhiC31 att recombination sites integrated into the chromosome. We then performed PCR on the wild-type and inverted strains using the four possible combinations to check the orientation of the piece in question. Note that there is no detectable band for the endogenous junctions in the inverted strain, indicating that there is no reversion to the wild-type chromosomal configuration.

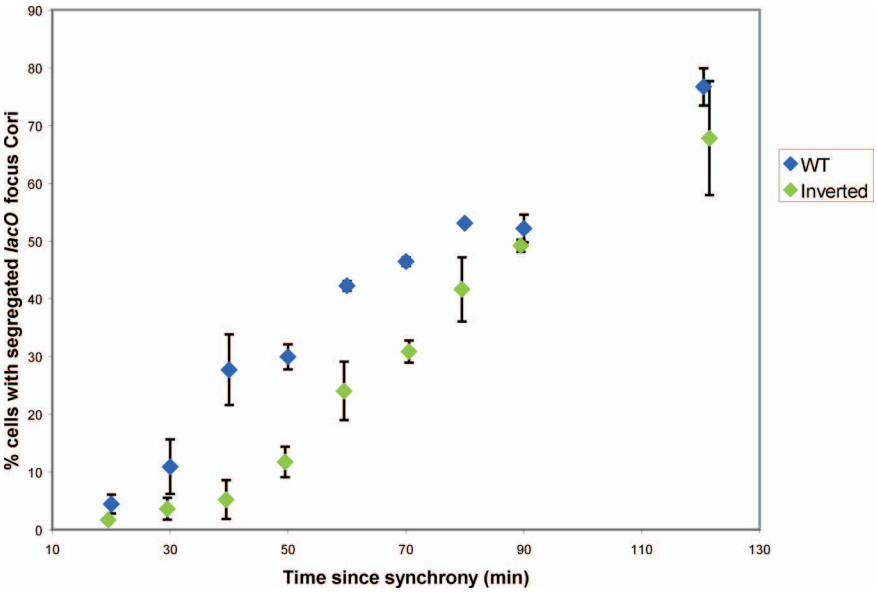

Fig. S4. Population segregation dynamics of *Cori* in wild-type and inverted strains/Plot of the percentage of cells with two distinct LacI-CFP foci as a function of time from synchrony. To avoid phototoxicity effects, a new field of cells was imaged for each timepoint. Chromosome configurations as in Fig. 2*D*. Symbols represent means of two experiments.

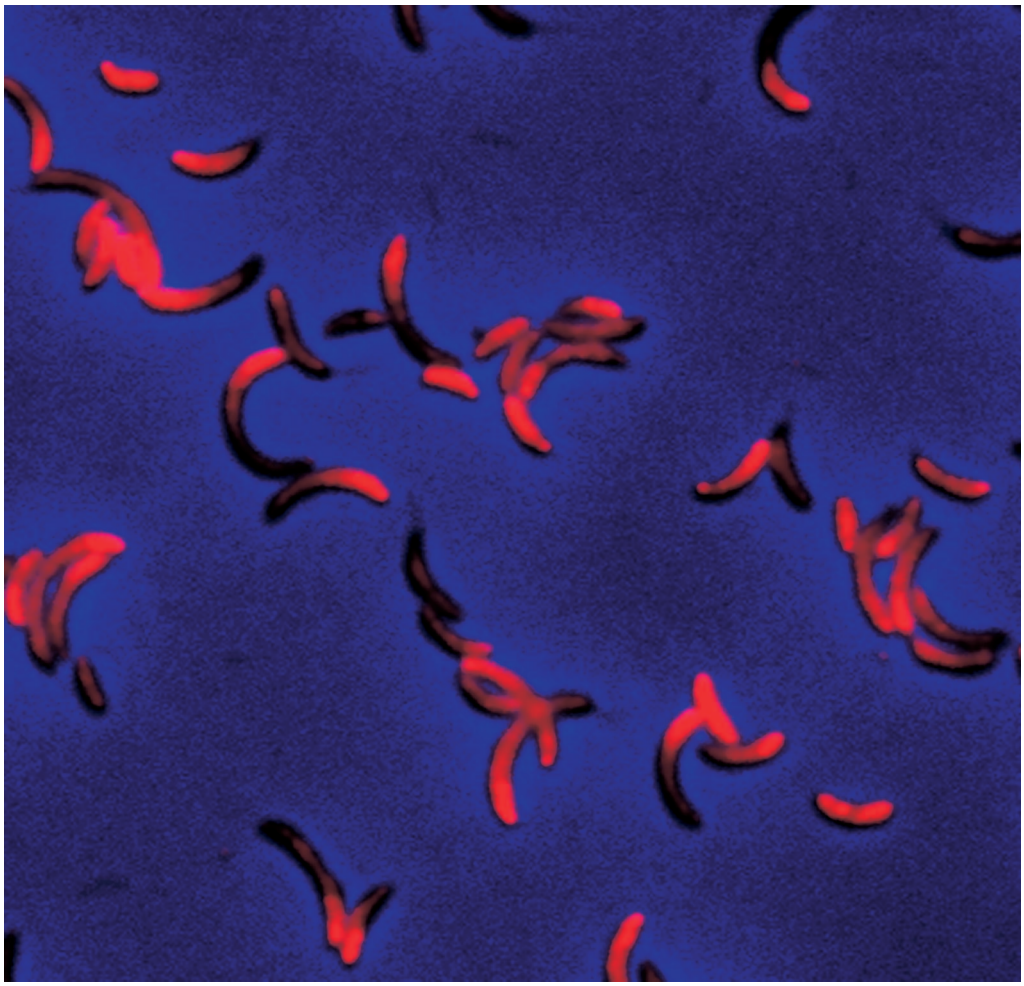

Fig. S5. - ParA-mCherry localization in strain ET225 after 5 h of induction with 0.3% xylose/ParA-mCherry fluorescence is pseudocolored red overlaid on a blue pseudocolored phase image to show the cell bodies.

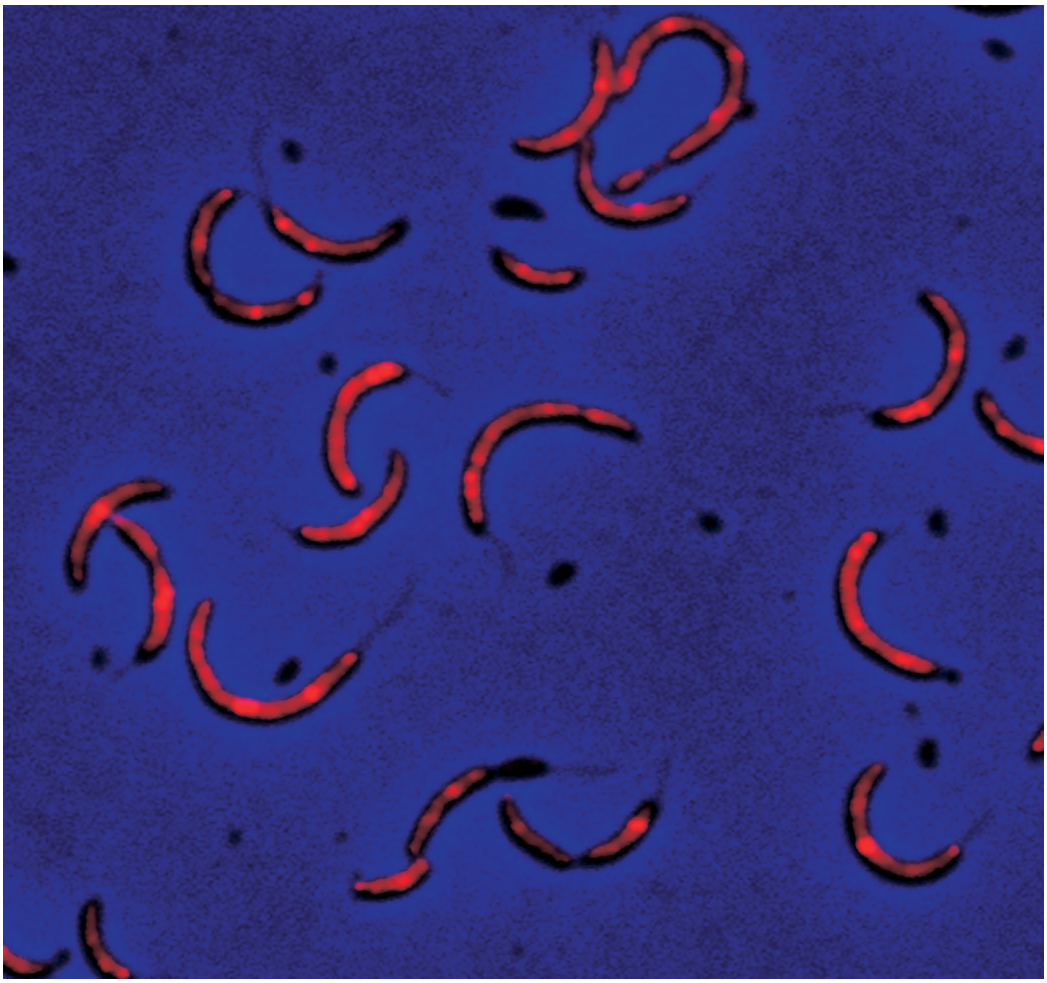

Fig. S6. - ParAK20R-mCherry localization after 5 h of induction with 0.3% xylose/ParAK20R-mCherry fluorescence is pseudocolored red overlaid on a blue pseudocolored phase image to show the cell bodies.

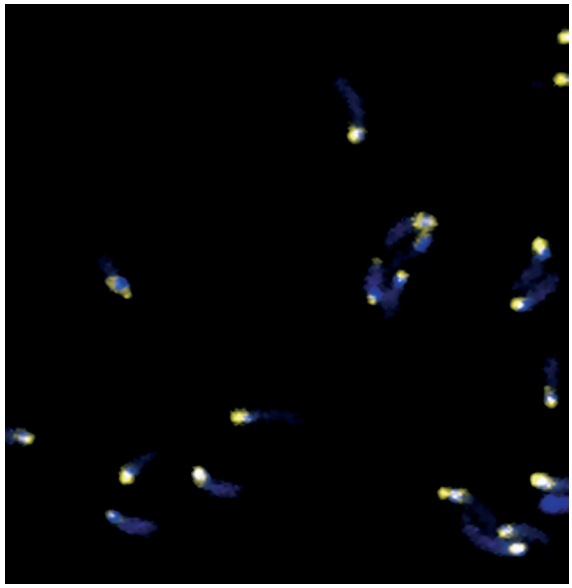

Movie S1. Segregation of *parS* and *lacO* at + 4 kb (cells from strain ET70). LacI-CFP expression was induced by addition of 0.03% xylose for 75 min. Pictures were taken every 4 min starting at $t = 20$ and ending at $t = 44$. LacI-CFP fluorescence was false colored blue; MipZ-YFP fluorescence was false colored yellow. Red ovals in first frame highlight cells that segregate during this time period.

Movie S1 (MOV)

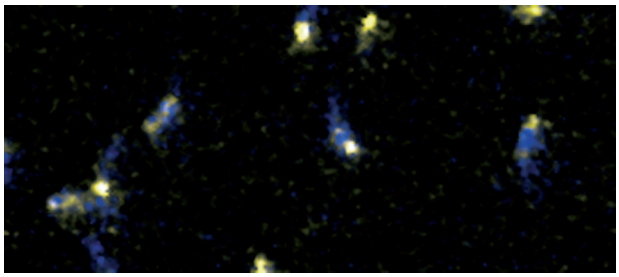

Movie S2. Segregation of *parS* and *parS*(pMT1) at −5 kb (cells from strain ET83). LacI-CFP expression was induced by addition of 0.03% xylose for 75 min. Pictures were taken every 5 min starting at $t = 20$ and ending at $t = 50$. CFP-pMT1Δ23ParB fluorescence was false colored blue; MipZ-YFP fluorescence was false colored yellow. White ovals in first frame highlight cells that segregate during this time period.

Movie S2 (MOV)

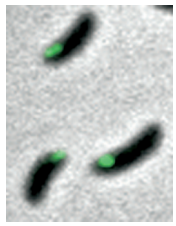

Movie S3. Segregation of ParB in cells expressing ParA-mCherry. Cells from strain ET228 were grown to mid logarithmic phase (O.D. < 0.3) and ParA-mCherry expression was induced by addition of 0.03% xylose for 60 min. Pictures were taken on the CFP channel every 10 min starting at $t = 20$ and ending at $t = 90$. ParB-CFP fluorescence was pseudocolored green and overlaid with blue-pseudocolored phase contrast images to show the cell bodies.

Movie S3 (MOV)

Movie S4. Segregation of ParB in cells expressing ParAK20R-mCherry. Cells from strain ET227 were grown to mid logarithmic phase (O.D. < 0.3) and ParAK20R-mCherry expression was induced by addition of 0.03% xylose for 60 min. Pictures of the CFP channel were taken every 10 min starting at $t = 20$ and ending at $t = 90$. ParB-CFP fluorescence was pseudocolored green and overlaid with blue-pseudocolored phase contrast images to show the cell bodies.

Movie S4 (MOV)

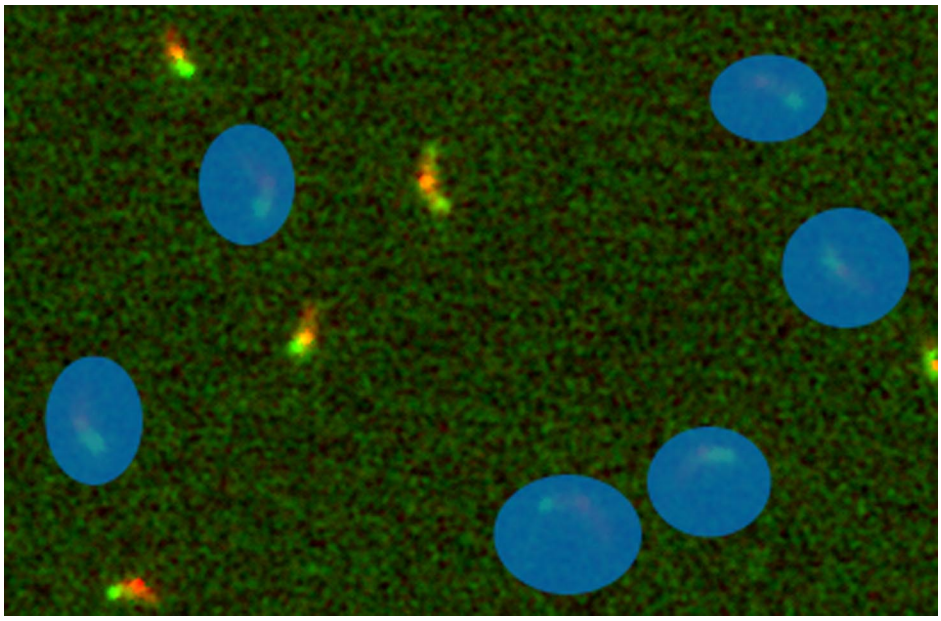

Movie S5. Segregation of *parS* and *lacO* at −44 kb in inverted strain ET153. LacI-CFP expression was induced by addition of 0.03% xylose for 75 min. Pictures were taken every 10 min from $t = 30$ to $t = 70$ and every 20 min thereafter ending at $t = 130$. LacI-CFP fluorescence was false colored red; MipZ-YFP fluorescence was false colored green. Blue ovals in first frame highlight cells that segregate during this time period.

Movie S5 (MOV)

Table S1. Plasmids

Figure	Plasmid name	Relevant features	Resistance marker	Method of construction
Fig. 1 *C* and *D*	pTORO37	parS WT	Chloramphenicol	Phosphorilated and hybridized primers 95 and 96, and ligated this into EcoRI-cut pMR31
Fig. 1 *C* and *D*	pTORO38	parS Mut	Chloramphenicol	Phosphorilated and hybridized primers 97 and 98, and ligated this into EcoRI-cut pMR31
Figs. 2 *D* and *E*, 4, and 5	pTORO78	PhiC31 recombinase under Pvan control	Chloramphenicol	Pvan-PhiC31 in pRVMCS-6

Table S2. Strains

Figure	Strain name	Resistance	Phenotype
Figs. 2*A*, 5*B*, S4	ET 70	Kan	Pxyl-LacI-CFP; PMipZ-MipZ-YFP; LacO arrays at + 4kb
Fig. 2*B*	ET 83	Kan, Gent	PMipz-MipZ-YFP; Pxyl CFP-ParB(pMT1); ParS(pMT1) at 4012 kb
Figs. 2 *C* and *E*, 5*A*	ET 147	Kan	Pxyl-LacI-CFP; PMipZ-MipZ-YFP; LacO at 3′953.270bp; attB at 3′908.000; attP at 4′012.500
Fig. 2*E*	ET 78	Kan, Chlor	Pxyl-LacI-CFP; PMipZ-MipZ-YFP; LacO at 3′913.719bp; Inversion of DNA between 3908 kb and 4004 kb.
Figs. 3, S6	ET 230	Kan, Tet	Pxyl-ParA-K20R-mCherry; PparB-CFP-ParB; Pvan-PopZ-YFP
Figs. 3, S5	ET 231	Kan, Tet	Pxyl-ParA-WT-mCherry; PparB-CFP-ParB; Pvan-PopZ-YFP
Figs. 4, 5*A*	ET 153	Kan, Chlor	Pxyl-LacI-CFP; PMipZ-MipZ-YFP; LacO at 3′953.270bp; Inversion of DNA between 3908 kb and 4012.5 kb
Figs. 5*B*, S4	ET160	Kan	Pxyl-LacI-CFP; PMipZ-MipZ-YFP; LacO arrays at + 4kb. Inversion of DNA between 3908 kb and 4012.5 kb
Fig. 5*B*	ET 172	Kan	Pxyl-LacI-CFP; PMipZ-MipZ-YFP; LacO arrays at + 4kb. Inversion of DNA between 3585 kb and 4012.5 kb
Fig. S1	ET150	Kan	Pmipz-MipZ-YFP; Pxyl CFP-ParB(pMT1)

Table S3. Primers

Primer number	Primer sequence
95	AATTCactcatcggcgtttcacgtgaaacacccccaccgcagctgtgagcggcctgtggacaatattggggatgttccacgtgaaacatcacttg
96	AATTCcaagtgatgtttcacgtggaacatccccaatattgtccacaggccgctcacagctgcggtgggggtgtttcacgtgaaacgccgatgagt
97	AATTCactcatcggcaaaacacgtgaaacacccccaccgcagctgtgagcggcctgtggacaatattggggataaaacacgtgaaacatcacttg
98	AATTCcaagtgatgtttcacgtgttttatccccaatattgtccacaggccgctcacagctgcggtgggggtgtttcacgtgttttgccgatgagt